Solar Physics (2025) 300:113
https://doi.org/10.1007/s11207-025-02518-9

RESEARCH

Ground-Level Enhancement of 8 June 2024 (GLE 75) Caused by Solar Energetic Particles

Stepan Poluianov[1,2] · Alexander Mishev[1,2] · Olga Kryakunova[3] · Botakoz Seifullina[3] · Nikolay Nikolayevskiy[3] · Ilya Usoskin[1,2]

Received: 11 February 2025 / Accepted: 8 July 2025

Abstract
Solar eruptive events such as flares and coronal mass ejections can accelerate charged particles up to nearly relativistic energies producing so-called solar energetic particles (SEPs). Some of those SEPs can propagate towards Earth and be registered by, e.g., particle detectors onboard satellites. Favourable acceleration conditions make strong SEP events possible with a high flux of high-energy (>500 MeV) protons, which can be registered even on the ground by neutron monitors (NMs) as rapid enhancements of their count rate over the background. Such events are accordingly called ground-level enhancements (GLEs). GLEs are rare, with only 73 events registered from 1942 to 2023, and three more GLEs 74 – 76 occurred in 2024, close to the maximum of solar activity. In this work, we report GLE 75 that happened on 8 June 2024, initially missed during real-time monitoring, but identified retrospectively. The SEP event, which induced the GLE, was associated with a flare from the solar active region 13697 (13664 on the previous solar rotation). It caused statistically significant increases in the count rate of NMs Dome C, South Pole, and Peawanuck, as well as in the proton intensity measured by Geostationary Operational Environmental Satellite GOES-16. Here, we show the GLE in NM data, describe the procedure of evaluation of its statistical significance, and present the analysis with reconstruction of the spectral and angular SEP distributions.

Keywords GLE · Ground-level enhancement · SEP · Solar energetic particles · Neutron monitor

1. Introduction

The high-energy particle radiation environment near the Earth is governed by the omnipresent galactic cosmic rays (GCRs) originating mostly from our Galaxy, yet the most energetic species have extra-galactic origin (e.g., Gaisser, Engel, and Resconi 2016). In addition, there are also the so-called solar energetic particles (SEPs) accelerated during solar

✉ S. Poluianov
stepan.poluianov@oulu.fi

1 Sodankylä Geophysical Observatory, University of Oulu, 90014 Oulu, Finland

2 Space Physics and Astronomy Research Unit, University of Oulu, 90014 Oulu, Finland

3 Institute of Ionosphere, 050020 Almaty, Kazakhstan

Published online: 18 August 2025

eruptive processes such as solar flares and coronal mass ejections (CMEs) (e.g., Reames 1995; Waterfall et al. 2023). SEPs have a sporadic nature, and occasionally can be observed in the vicinity of the Earth, as well as at other locations in the Heliosphere (e.g., Guo et al. 2023). Here we focus on a specific class of SEPs, that can be observed on the surface of the Earth, namely the ground-level enhancements, details given below.

Naturally, SEP events can differ from one to another by their acceleration sites, heliospheric conditions, and connectivity to the Earth, resulting in their spatial distribution, duration, energy ranges and intensities of particles (Miroshnichenko 2015, 2018). Therefore, they are studied on a case-by-case basis.

SEPs are routinely studied with space-borne instruments and ground-based detectors at the Earth. Spacecraft provide direct measurements of the SEP intensity, whilst ground-based observations specifically with neutron monitors (NMs) register SEPs indirectly via detection of secondary hadrons from cosmic-ray induced atmospheric cascades (e.g. see, Simpson 2000; Dorman 2004, and references therein). Both approaches have their own advantages and disadvantages and are complement to each other (e.g., Tylka and Dietrich 2009; Raukunen et al. 2018; Koldobskiy et al. 2021). In this work, we employ mostly ground-level measurements with NMs.

An SEP event in NM data is observed as an enhancement of the count rate over the GCR-defined background and accordingly called a Ground-Level Enhancement (GLE). By definition, a GLE is registered when there are statistically significant enhancements in the count rates of at least two NMs in different locations. The solar origin should be confirmed by a corresponding increase in the particle intensity directly measured by space-borne instrument(s) (Poluianov et al. 2017). NM stations at different locations have different geomagnetic and atmospheric cutoffs (latitude- and altitude-dependent, respectively) and thus accordingly different sensitivity to register SEPs (e.g., Smart and Shea 2009; Mishev and Poluianov 2021; Poluianov and Batalla 2022). This gives the necessary basis to study SEPs, namely by using the global network of NMs as a single giant spectrometer (Bieber and Evenson 1995; Mishev and Usoskin 2020).

Since 1942, there were 75 known GLEs including two events registered on 11 May 2024 and 21 November 2024. Starting from GLE 5, they can be found in the International GLE Database at https://gle.oulu.fi. However, after careful re-examination of existing data, we found one more GLE that happened on 8 June 2024 and was associated with a very productive solar active region that generated multiple X-class flares, caused strong geomagnetic storms and GLE 74 in May 2024. In this work, we report the newly found GLE named number 75, describe the evaluation procedure of the statistical significance of an NM count rate enhancement needed to claim a GLE, and present an analysis of the event with a reconstructed energy and angular distributions of SEPs that caused it.

2. Observations

Herein we used records from 16 polar NM stations, shown in Figure 1, details given in Table 1. The NM count rates were mainly retrieved from the Neutron Monitor Database NMDB (https://www.nmdb.eu). SNAE data were provided by the station PI. For BRBG and NRLK, we used the plots from the database of the Pushkov Institute of Terrestrial Magnetism, Ionosphere and Radio Wave Propagation (IZMIRAN, http://cr0.izmiran.ru/common/links.htm). Data from OULU, DOMB and DOMC NMs were directly taken from the Oulu cosmic-ray database at https://cosmicrays.oulu.fi/. We used data with a 5-minute

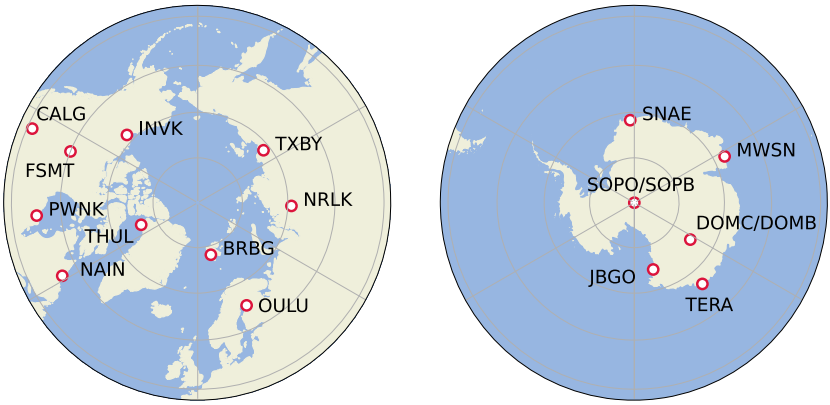

Figure 1 Map with locations of NM stations used in this work. The northern and southern polar regions are on the left- and right-hand sides, respectively. See Table 1 for details.

Table 1 NM stations used in this work. The type NM64 is the standard design described by Carmichael (1964), while the compact type mini-NM is presented in Poluianov et al. (2015), Strauss et al. (2020). The information about the stations was taken from databases NMDB (https://www.nmdb.eu), IZMIRAN (http://cr0.izmiran.ru/common/links.htm), and https://pgia.ru/data/nm. The elevation is given in meters above sea level (m asl). The geomagnetic cutoff rigidity R_c was computed specifically for the GLE time with code OTSO (Larsen, Mishev, and Usoskin 2023). The confidence interval of the integral increase C_{cum} is given for 3 standard deviations.

Name	Abbreviation	NM type	Elevation (m asl)	Geom. cutoff R_c (GV)	Increase C_{cum} (% h)
Barentsburg	BRBG	18NM64	70	0.0	0.0*
Dome C	DOMC	mini-NM	3233	0.0	3.04 ± 1.97
Calgary	CALG	12NM64	1128	0.9	0.49 ± 0.62
Fort Smith	FSMT	18NM64	180	0.2	-0.04 ± 0.79
Inuvik	INVK	18NM64	21	0.2	0.93 ± 1.00
Jang Bogo	JBGO	6NM64	30	0.0	0.97 ± 0.89
Mawson	MWSN	18NM64	30	0.4	1.02 ± 0.53
Nain	NAIN	18NM64	46	0.2	0.68 ± 0.87
Norilsk	NRLK	18NM64	0	0.4	0.0*
Oulu	OULU	9NM64	15	0.4	0.78 ± 1.43
Peawanuck	PWNK	18NM64	53	0.2	1.54 ± 1.04
SANAE IV	SNAE	6NM64	856	0.3	1.26 ± 1.18
South Pole	SOPO	3NM64	2820	0.0	2.03 ± 0.59
Terre Adelie	TERA	9NM64	30	0.0	-0.10 ± 0.97
Thule	THUL	18NM64	26	0.0	0.92 ± 0.88
Tixie Bay	TXBY	18NM64	0	0.5	0.25 ± 0.94

*The count rate increase was assessed from a plot

time resolution as a good compromise between the reduced random variability of the signals and still sufficiently fine resolution. Most of the NMs listed in Table 1 are standard instruments of the type NM64 described in Carmichael (1964). However, DOMC has the

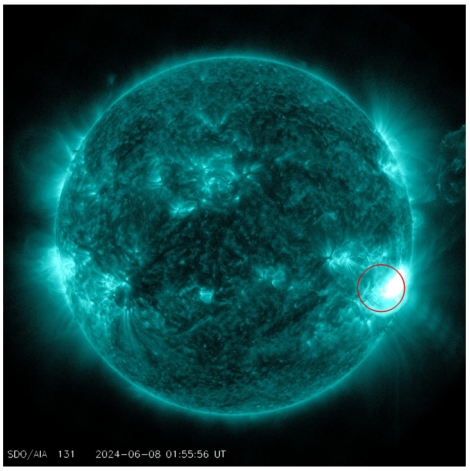

Figure 2 Eruption at the Sun as captured in the Solar Dynamics Observatory extreme ultraviolet filtergrams at 131 Å and associated to the active region 13697 (encircled in the image). The figure corresponds to 01:55:56 UT, 8 June 2024. Adopted from https://www.spaceweatherlive.com/en/archive/2024/06/08/xray.html.

"mini-NM" design (Poluianov et al. 2015; Strauss et al. 2020). In addition to those instruments, there are so-called "bare", i.e., having no lead layer NMs DOMB and SOPB in the same locations as DOMC and SOPO, respectively. We excluded them from the analysis due to the lack of a reliable yield function, but still find it useful to show their behaviour during the GLE, see Figures 3 and 7.

To confirm the arrival of SEPs to the Earth, we used the proton intensity data measured by a particle detector onboard the Geostationary Operational Environmental Satellite GOES-16 with the 5-minute resolution. This data are available on the website of the National Centers for Environmental Information of the U.S. National Oceanic and Atmospheric Administration (https://data.ngdc.noaa.gov).

On 8 June 2024, the solar active region 13697 has been relatively quiet, however approaching the western limb of the Sun, it produced a long-duration flare classified with the soft X-ray intensity as M9.7 (Figure 2). The flare had the onset at 01:23 UT, reached the maximum at 01:49 UT and ended at 02:19 UT. It was accompanied by a coronal mass ejection (https://kauai.ccmc.gsfc.nasa.gov/CMEscoreboard/). We note that a smaller eruption of M3.3 occurred an hour earlier, at 00:51 UT. The M9.7 flare and the following CME produced SEPs that reached the Earth at around 02:00 UT, as seen in the proton intensity data from GOES-16 (Figure 3 (c) and (d)).

The NM count rates, normalized to the background but not detrended, are shown in Figure 3 (a) and (b). Their backgrounds used for normalization and thus corresponding to 0% were calculated as the average count rates during two hours before the SEP event, specifically, during 00:00 – 02:00 UT, 8 June 2024. In order to highlight the timing of the SEP event in the figure, we added a vertical arrow indicating the maximum of the solar flare and plotted the proton intensity for energies $E > 500$ MeV measured by GOES-16 (Figure 3 (c) and (d)).

A visual comparison of the count rate series and the proton intensity from GOES provided us with initial hints that SOPO, SOPB, and PWNK observed increases during the SEP event. DOMC and especially DOMB have very high variability of the data, which is explained by their compact mini-NM design and consequent low count rates. For a further, more robust evaluation of the increases, we detrended data and calculated the count rate cumulative sums $C_{\mathrm{cum}}(t)$ for every NM series and corresponding errors (cf. Usoskin et al. 2020). Based on that, the time-integral increases were estimated, and their values and confidence intervals at the level of $3\sigma_{\mathrm{cum}}$ are given in Table 1. Additionally, it was clarified

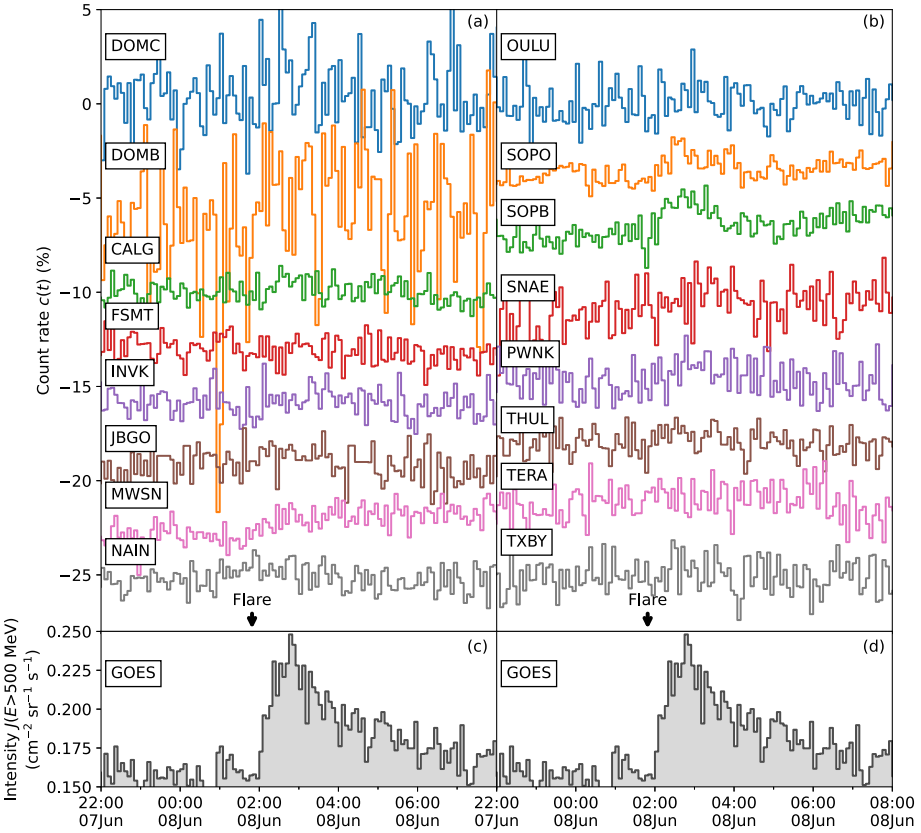

Figure 3 NM count rates (panels (a) and (b)) and the proton intensity for $E > 500$ MeV from satellite GOES-16 (panels (c) and (d)) during the GLE. The NM count rates are given normalized to corresponding average values during 2 hours before the event (00:00 – 02:00 UT, 8 June 2024) and with offsets for better visibility. The time of the associated solar flare's maximum is marked by a vertical arrow. Panels (c) and (d) are identical. The time in the x-axis is given in UT.

from the $C_{\rm cum}(t)$ curves that the GLE event had the onset at 02:00 UT and ended at 04:10 UT. The details of the calculations are described in the Appendix. The integral increases ranged from null in most NM data up to $3.04 \pm 1.97\%$ h in DOMC. Here, we considered an increase as null, if it did not exceed its confidence interval, i.e., was not statistically significant. Therefore, we concluded that three NM stations did statistically significant responses in $C_{\rm cum} \pm 3\sigma_{\rm cum}$ during the SEP event: DOMC ($3.04 \pm 1.97\%$ h), PWNK ($1.54 \pm 1.04\%$ h), and SOPO ($2.03 \pm 0.59\%$ h). Their data are shown in more detail in Figure 4. There are also stations JBGO, SNAE, THUL, which showed marginally significant increases but were conservatively assumed by us as having null responses. Also, we decided to take the station MWSN as null because of its quite small increase, though it was formally significant ($1.02 \pm 0.53\%$ h). Then, BRBG, CALG, FSMT, INVK, NAIN, NRLK, OULU, TERA, and TXBY had clearly no statistically significant increases. The "bare" NMs DOMB and SOPB had also very noticeable enhancements of the count rate of 4.80 ± 5.41 and $2.20 \pm 0.76\%$ h, respectively. DOMB, though having the highest increase among all NMs, did not have it statistically significant due to a very low count rate, approximately 250 counts min^{-1}. The

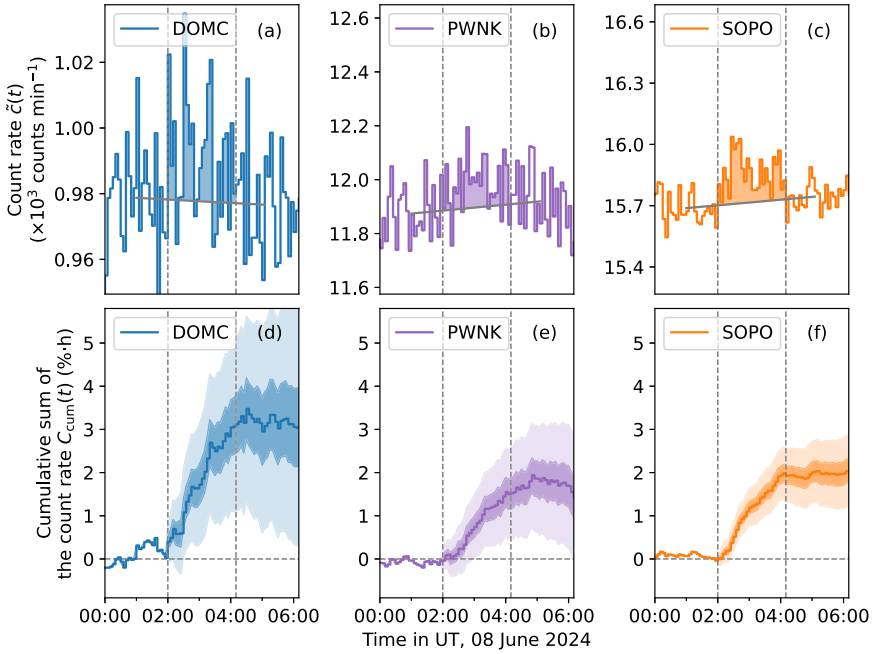

Figure 4 Count rates $\tilde{c}(t)$ (in $\times 10^3$ counts min^{-1}) of DOMC, PWNK, and SOPO during the GLE on 8 June 2024 (panels (a), (b), and (c), respectively). The enhancements associated with the event are highlighted with colour-filled areas. The solid grey lines indicate the linear background interpolations derived from 2-hour periods before and after the GLE and used for detrending. Panels (d), (e), and (f) show the calculated cumulative sums of the count rates $C_{\mathrm{cum}}(t)$ of DOMC, PWNK, and SOPO, respectively. The 1σ and 3σ error bands are shown with dark and light colour areas. The onset and end of the studied increase are marked with vertical dashed lines.

agreement in timing of the observed NM count rate enhancements, increase of the proton intensity measured by GOES, and the M9.7 solar flare support the conclusion that the NM count rate enhancements were caused by SEPs, and thus there was a GLE on 8 June 2024 according to its definition (Poluianov et al. 2017).

3. Analysis

To assess the characteristics of SEPs, causing the GLE event on 8 June 2024, we collected and analysed different data sets. The ground-based records analysis involves both modelling of the magnetospheric propagation of particles and the detector's response, including unfolding of spectral and angular information of solar protons for the latter (for details see Bütikofer 2018a,b, and references therein).

In order to analyse the characteristics of a strong SEP event, it is necessary to model accurately the magnetospheric conditions, specifically to compute the cutoff rigidity and asymptotic directions of NM stations. Herein, a recently developed tool OTSO was used, its full description is given in Larsen, Mishev, and Usoskin (2023). Since the K_{p} index prior to the event was below 5, we employed a combination of the International Geomagnetic Reference Field IGRF-13 (Alken et al. 2021) as the internal, and Tsyganenko-89 (Tsyganenko

1989) as the external field, which provides reliable approach for an undisturbed geomagnetosphere (e.g. Kudela, Bučik, and Bobik 2008; Larsen, Mishev, and Usoskin 2023).

The spectra and anisotropy of the GLE-causing SEPs can be derived using a method based on the modelling of the global NM response (Mishev 2023). In this study, we employed the approach adapted from the algorithm proposed by Cramp et al. (1997), subsequently used by different teams, e.g. by Bombardieri et al. (2006) and Vashenyuk et al. (2006). The applied here method is described elsewhere (Mishev et al. 2021), yet a slight modification related to the quality of the fit (see their Section 4.3 in Mishev et al. 2024) is introduced that accounts for the specifics of the GLE analysis when there is a marginal count rate increase of the majority of NM stations (for details see Poluianov et al. 2024).

In general, the method consists of modelling of the global NM response and subsequent unfolding of the spectra by several steps: computation of geomagnetic cutoff rigidities and asymptotic directions of all NMs, and a least-squares optimization of the difference between experimental and modelled NM responses. We emphasize that the modelling procedure should reproduce the observed increases as well as zero/marginal NM responses (Cramp et al. 1997; Mishev et al. 2024). Records from stations with a null count rate increase determine the boundary on SEP spectra and anisotropy. Therefore, the inclusion of stations such as BRBG and TXBY, which revealed zero count rate increases in their 1-hour data, is justified.

We note that a natural initial guess for the optimization is assumed, that is, plausible spectra and angular distribution based on statistical analysis of a plethora of GLEs (Kocharov et al. 2023; Larsen and Mishev 2024) and assuming the apparent source position along the interplanetary magnetic field (Mishev and Usoskin 2016b; Kocharov et al. 2017), herein retrieved from space-borne measurements by Advanced Composition Explorer (ACE, Smith et al. 1998). The modelling employs a new-generation NM yield function (for details see Mishev et al. 2020) calibrated on direct particle measurements with PAMELA (Payload for Antimatter Matter Exploration and Light-nuclei Astrophysics, Adriani et al. 2017) and AMS-02 (Alpha Magnetic Spectrometer, Aguilar et al. 2021) space-borne experiments (for details see Koldobskiy et al. 2019; Koldobskiy and Mishev 2022, and the discussion therein). The new NM yield function is also in very good agreement with latitude surveys and was recommended for GLE analysis (e.g. Nuntiyakul et al. 2018; Xaplanteris et al. 2021; Caballero-Lopez and Manzano 2022).

There are several criteria that determine the quality of the fit, governed by the normalized residual (e.g. Himmelblau 1972; Dennis and Schnabel 1996), see Equation 1, uniform distribution of the normalized residual, targetting relative difference between the observed and calculated NM increases to be about 10 – 15% for each NM with statistically significant count rate increase and avoiding over-fitting (Aster, Borchers, and Thurber 2005).

The merit function $\mathcal{D}$ is defined as

$$\mathcal{D} = \frac{\sqrt{\sum_{i=1}^{m}\left[\left(\frac{\Delta N_i}{N_i}\right)_{\mathrm{mod}} - \left(\frac{\Delta N_i}{N_i}\right)_{\mathrm{meas}}\right]^2}}{\sum_{i=1}^{m}\left(\frac{\Delta N_i}{N_i}\right)_{\mathrm{meas}}}, \tag{1}$$

where $\left(\frac{\Delta N_i}{N_i}\right)_{\mathrm{mod}}$ and $\left(\frac{\Delta N_i}{N_i}\right)_{\mathrm{meas}}$ are the modelled and measured relative count rate increases of the i^{th} NM, respectively, and m is the number of the stations used in the analysis, herein used only the polar stations possessing a greater response to SEPs (Bieber and Evenson 1995).

A reliable fit is achieved, with sustainable and smooth convergence of the optimisation, leading to a robust solution and satisfactory fit of the experimental data, when $\mathcal{D} \leq 5 - 10\%$

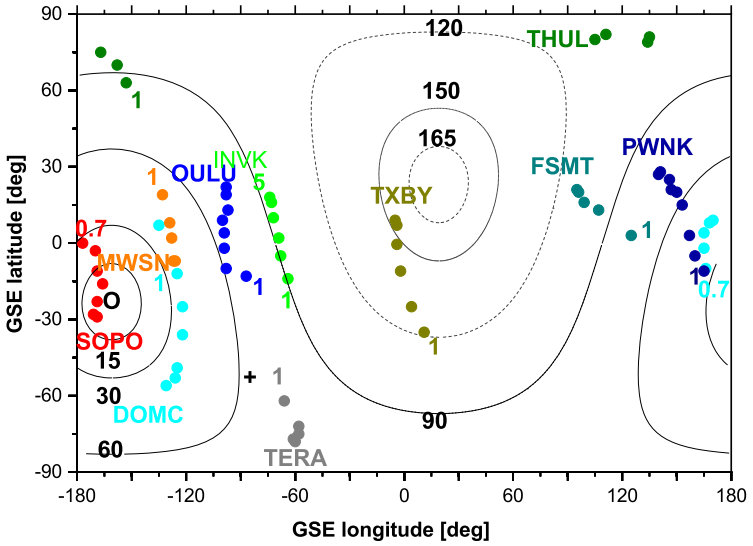

Figure 5 Selected asymptotic directions of polar NM stations during the GLE event of 8 June 2024 at 02:00 UT. The asymptotic directions are shown as dots, different colours for different NMs. Each series is plotted for protons of rigidities from the atmospheric cutoff (~ 1 GV for sea level) to 5 GV with an exception for high-altitude SOPO and DOMC having the rigidity range 0.7 – 5 GV. The small black circle depicts the derived anisotropy axis direction, while the cross corresponds to the interplanetary magnetic field direction according to measurements from the satellite Advanced Composition Explorer (ACE, Smith et al. 1998). The lines of equal pitch angles relative to the derived anisotropy axis are plotted for 15°, 30°, 60°, and 90° for the sunward direction, and 120°, 150°, and 165° for the anti-Sun direction. The coordinate system of the figure is Geocentric Solar Ecliptic (GSE).

(Vashenyuk et al. 2006; Mishev and Usoskin 2016a), however $\mathcal{D}$ could be $\approx 15 - 20\%$ for weak GLEs (e.g. Dennis and Schnabel 1996; Mishev et al. 2018), still providing reasonable results. Herein, the optimisation procedure uses the Levenberg-Marquardt algorithm (Levenberg 1944; Marquardt 1963) and includes also the ridge regression (Tikhonov et al. 1995; Johansen 1997; Leonov and Yagola 1998; van Wieringen 2015; Huber 2019), allowing to unfold the SEP spectra in a case, when marginal NM count rate increases are considered in the analysis (Engl, Hanke, and Neubauer 1996; Yagola, Leonov, and Titarenko 2002).

4. Results and Discussion

A moderate interplanetary disturbance was observed prior to the event, yet the geomagnetospheric conditions during the GLE on 8 June 2024 were relatively quiet with K_p index of about 4 (Matzka et al. 2021, https://kp.gfz-potsdam.de/en/data). This resulted on straightforward modelling of proton propagation in the magnetosphere using OTSO with IGRF-13 (epoch 2020) as the internal field model and the Tsyganenko-89 model as the external field. Several computed asymptotic directions for selected NM stations are shown in Figure 5 as an illustration. We point out that we plot asymptotic directions in the maximum NM response range of 1 – 5 GV (0.7 – 5 GV for the high-altitude stations SOPO and DOMC) in the figure, whilst the broader rigidity range of 1 – 20 GV (0.7 – 20 GV for SOPO and DOMC) was used in the analysis.

Table 2 Derived characteristics of SEPs during the GLE event on 8 June 2024. The spectral shape with parameters j_0, γ, $\delta\gamma$, and angular distribution with parameter s^2 according to Equations 2 – 3 are presented with the 95% confidence intervals. The fit merit function $\mathcal{D}$ (see Equation 1) in the corresponding range, the geographical latitudes Ψ and longitudes Λ of the anisotropy axis positions are also shown. The accuracy of the derived Ψ and Λ is in the range of $\pm$ 8 – 12 degrees.

Interval (UT)	j_0 (cm^{-2} sr^{-1} s^{-1} GV^{-1})	γ	$\delta\gamma$ (GV^{-1})	s^2 (rad^2)	Ψ (deg)	Λ (deg)	$\mathcal{D}$ (%)
02:00 – 02:15	$7.35^{+0.3}_{-0.1}$	$6.6^{+0.1}_{-0.1}$	0.7 ± 0.03	6.9 ± 0.2	− 12	− 161	9 – 12
02:15 – 02:30	$7.54^{+0.2}_{-0.3}$	$6.63^{+0.1}_{-0.1}$	0.65 ± 0.07	7.2 ± 0.1	− 17	− 165	11 – 15
02:30 – 02:45	$7.81^{+0.3}_{-0.2}$	$6.7^{+0.1}_{-0.1}$	0.6 ± 0.03	7.4 ± 0.1	− 23	− 171	12 – 14
02:45 – 03:00	$7.28^{+0.4}_{-0.3}$	$6.8^{+0.1}_{-0.1}$	0.6 ± 0.06	7.6 ± 0.3	− 31	− 173	9 – 12
03:00 – 03:15	$6.83^{+0.4}_{-0.2}$	$6.9^{+0.1}_{-0.1}$	0.6 ± 0.05	7.8 ± 0.2	− 25	− 178	8 – 12
03:15 – 03:30	$6.64^{+0.3}_{-0.4}$	$7.0^{+0.1}_{-0.1}$	0.6 ± 0.03	7.9 ± 0.3	− 20	174	10 – 13
03:30 – 03:45	$6.13^{+0.3}_{-0.1}$	$7.1^{+0.1}_{-0.1}$	0.6 ± 0.05	8.2 ± 0.1	− 21	172	8 – 10
03:45 – 04:00	$5.92^{+0.4}_{-0.2}$	$7.1^{+0.1}_{-0.1}$	0.6 ± 0.04	8.7 ± 0.4	− 17	169	7 – 9

A modified power-law function was applied to represent the SEP spectrum over a range of particle rigidities R (in GV):

$$j_{\parallel}(R) = j_0 R^{-(\gamma + \delta\gamma(R-1\,\mathrm{GV}))}, \tag{2}$$

where $j_{\parallel}(R)$ is the differential SEP intensity parallel to the axis of symmetry with geographic coordinates Ψ and Λ (see Table 2) and j_0 is the differential SEP intensity for rigidity $R = 1$ GV. Both $j_{\parallel}(R)$ and j_0 are in the units of particles cm^{-2} sr^{-1} s^{-1} GV^{-1}. Then, γ and $\delta\gamma$ are the power-law exponent (dimensionless) and its steepening (in GV^{-1}), respectively.

The SEP population was assumed to have some degree of anisotropy. For that, the particle angular distribution was approximately defined as a Gauss function:

$$G(\alpha) \sim e^{-\alpha^2/s^2}, \tag{3}$$

where α is the pitch angle, sic. the angle between the axis of symmetry of the particle distribution and the asymptotic viewing direction at rigidity R, associated with the arrival direction (Cramp et al. 1997; Bombardieri et al. 2008), and s is angular width of the distribution (both in radians).

The mentioned parameters of the SEP rigidity (energy) and angular distributions j_0, γ $\delta\gamma$, and s were reconstructed by minimising the merit function $\mathcal{D}$ and are presented in Table 2. One can see the temporal evolution of the SEP spectrum during the GLE with 15-minute averaging in Figure 6. The SEP spectrum was the most intensive and hard in the early phase of the GLE (02:00 – 03:00 UT), which is reflected in the high values of j_0 and low values of γ. The peak particle intensity was reached at about 02:30 UT. Accordingly, the second half of the GLE (03:00 – 04:00) was characterised by the decreasing intensity. A gradual softening of the spectrum (increase of γ) was observed during the event along with the particle pitch-angle distribution becoming slightly more isotropic (a small yet notable increase of s). Such an evolution is typical for many GLE and sub-GLE events (for example,

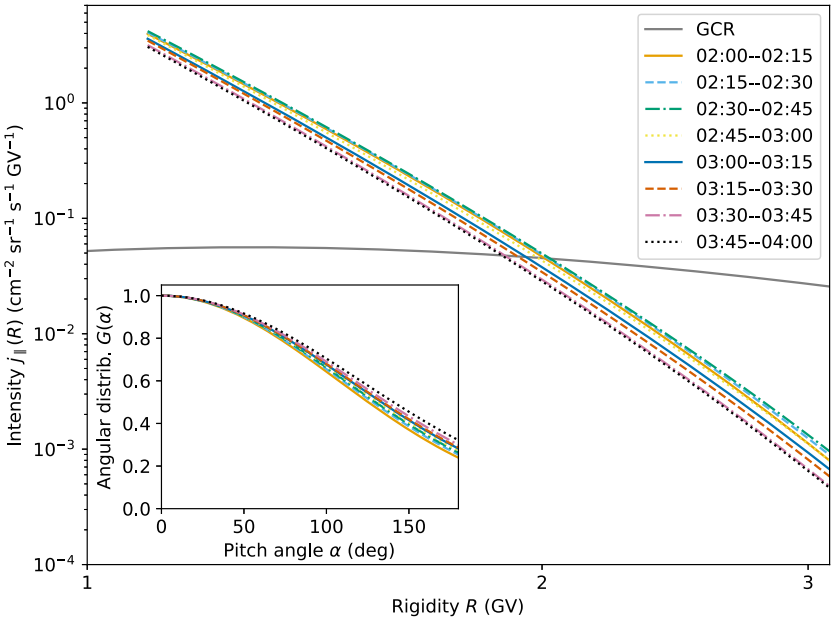

Figure 6 Reconstructed SEP differential intensity $j_{\parallel}(R)$ for 15-minute intervals during the GLE event plotted with the parameters from Table 2. The grey solid line indicates the GCR background as a reference. It corresponds to the solar modulation conditions of June 2024 ($\phi = 766$ MV, Usoskin et al. 2017). The inner panel shows the angular distribution of SEP during the event, the line styles are the same as in the main panel. The time intervals in the legend are given in UT.

Mishev et al. 2022, 2024; Hayakawa et al. 2024; Poluianov et al. 2024). Overall, the GLE 75 was very weak, close to the NM network detection limit and thus seen just by very few stations all over the world. However, it still satisfied the formal criteria of the GLE definition (Poluianov et al. 2017) and, thus, is considered a GLE, and reporting it is important for studies of the GLE occurrence statistics.

5. Summary

We reported a new GLE registered by NM stations Dome C, Peawanuck, and South Pole on 8 June 2024. The enhancement in the NM count rates happened right after a strong solar flare classified as M9.7 and coincided with the increase of the proton intensity measured by the particle detector onboard the satellite GOES-16. The maximum time-integrated and statistically significant increase was registered by DOMC as $3.04 \pm 1.97\%$ h. Using NM count rates from 16 stations, the SEP energy and angular distributions were reconstructed by solving the inverse problem with standard GLE analysis methods. The differential spectra and angular distributions for 15-minute intervals were presented in Figure 6 and Table 2. The GLE on 8 June 2024 got the number 75, and the NM data for it are available on the International GLE Database at https://gle.oulu.fi.

GLEs including small ones are related to relatively rare, strong, and hard-spectrum SEP events, which occur roughly several times per solar cycle. Due to the high diversity and relative rarity of such SEP events, studying small GLEs is valuable, as this improves the

statistics about GLEs, and enhances our understanding of SEP acceleration, propagation and interaction with the Earth.

Appendix

The statistical significance of an increase in the NM count rate was evaluated as described below.

In the first step, the data series were inspected for a background trend during the SEP event. If the trend exists, detrending is needed, which is usually done by approximating the background during the event with a polynomial or exponent. In this work, we used a linear function (the first-degree polynomial) for this purpose (see Figure 4), but the approach can significantly vary in other cases (Usoskin et al. 2020). The detrended data for many GLEs are available at the International GLE Database (https://gle.oulu.fi). As the next step, we used the detrended count rate $\tilde{c}(t)$ with the absolute units of counts min^{-1} and normalised it to the background thus obtaining the count rate $c(t)$ in per cent:

$$c(t) = \frac{\tilde{c}(t) - \overline{c_{\mathrm{bg}}}}{\overline{c_{\mathrm{bg}}}} \cdot 100\%, \tag{4}$$

The background count rate $\overline{c_{\mathrm{bg}}}$ in counts min^{-1} was defined as the average detrended count rate during the two-hour pre-event period. The standard deviation of the count rate σ (in %) was assumed to be the same for every data point during the whole studied period. It was estimated from the pre-event time interval as

$$\sigma = \sqrt{\frac{\sum_{i=1}^{N} c(t_i)^2}{N-1}}. \tag{5}$$

Specifically here, $c(t_i)$ is the normalized count rate in % for a given moment of time t_i during the pre-event interval and N is the number of data points there. We note that this approach makes sense for the count rate with a sufficiently high time resolution (1 – 5 minute data) providing N equal to least several tens.

Then, the cumulative sum of the count rate $C_{\mathrm{cum}}(t)$ in % h was calculated starting several hours before the event and ending several hours after it (see Figure 7):

$$C_{\mathrm{cum}}(t) = dt \sum_{k=t_0}^{t} c(k), \tag{6}$$

where dt is the time resolution (time step) in hours. The uncertainty of the cumulative sum $\sigma_{\mathrm{cum}}(t)$ with units % h can be calculated as:

$$\sigma_{\mathrm{cum}}(t) = dt \sqrt{\sum_{k=t_0}^{t} \sigma^2}. \tag{7}$$

Figure 7 shows the behaviour of the cumulative sum $C_{\mathrm{cum}}(t)$ over time for most NMs used in this work during the GLE. It fluctuates around zero before the increase (the first vertical dashed line), but then starts to grow as the increased count rate data points sum up. When the increase is over (the second dashed line), $C_{\mathrm{cum}}(t)$ flattens, but the uncertainties

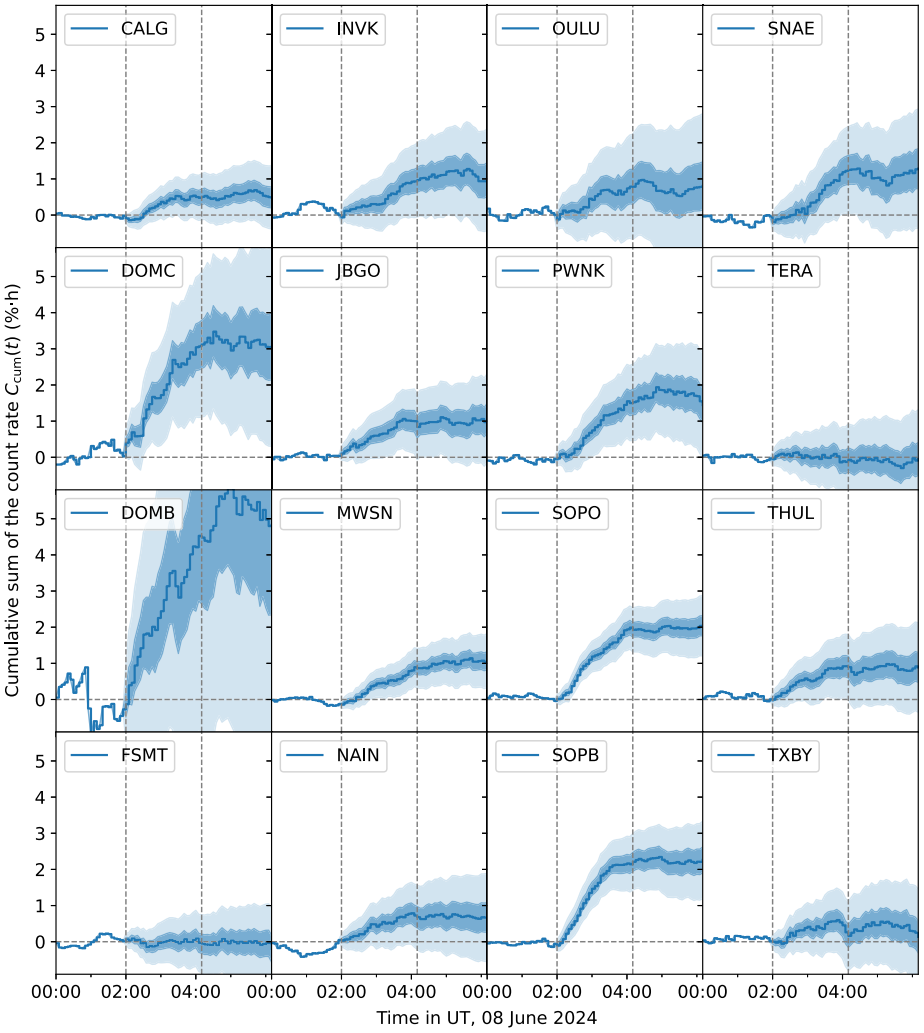

Figure 7 Cumulative sum of the count rate $C_{\mathrm{cum}}(t)$ for evaluation of the statistical significance of the increase. Each panel corresponds to one NM with its name given in the legend. The 1σ and 3σ error bands are shown with dark blue and light blue areas. The onset and end of the studied increase are marked with vertical dashed lines.

keep growing. The difference between $C_{\mathrm{cum}}(t)$ before and after the studied increase is the magnitude of the event observed by the given NM in % h. We consider the increase as statistically significant, if it exceeds 3 standard deviations, viz. $C_{\mathrm{cum}} > 3\sigma_{\mathrm{cum}}$.

Acknowledgments We warmly appreciate the work of PIs and colleagues from the NM community providing the data used in this paper, namely those managing the stations BRBG, CALG, FSMT, INVK, JBGO, MWSN, NAIN, NRLK, PWNK, SNAE, SOPO/SOPB, TERA, THUL, and TXBY. The Neutron Monitor Database NMDB (http://www.nmdb.eu) in Kiel, Germany founded under the European Union's FP7 programme (contract No. 213007), the U.S. NOAA, NASA, Solar Dynamics Observatory as well as IZMIRAN (Troitsk, Russia) are acknowledged for the data provided. Data of OULU, DOMB and DOMC are available at https://cosmicrays.oulu.fi/. We acknowledge the Italian polar program PNRA (via the AIR-FLOC PNRA

OSS-04 project), the French Polar Institute IPEV and the Finnish Antarctic Research Program (FINNARP) for hosting DOMC/DOMB neutron monitors at station Concordia.

Author Contributions S.P. did data processing including evaluation of the statistical significance of the results, made Figures 1, 3, 4, 6, 7 and Table 1, and coordinated the work of all co-authors; A.M. analysed the event and reconstructed the properties of solar energetic particles that caused it, also made Figure 5 and Table 2; O.K. and N.N. discovered the event and conceived the idea of this work; B.S. contributed with the solar flare data and space weather prior and during the event (including Figure 2). I.U. provided the main input into the method of evaluation of the statistical significance of the results. S.P. and A.M. were the main writers, but all authors notably contributed to the manuscript with text, tables and/or plots. All authors reviewed the manuscript.

Funding Information Open Access funding provided by University of Oulu (including Oulu University Hospital). This research is funded by the Committee of Science of the Ministry of Science and Higher Education of the Republic of Kazakhstan (Grant No. AP23489700). This study was partly supported by the Research Council of Finland project No. 354280 GERACLIS and the Horizon Europe Program projects ALBATROS and SPEARHEAD. We benefited from the support of the International Space Science Institute (Bern, Switzerland) project No. 585 REASSESS and from the partial support of the National Science Fund of Bulgaria under contract KP-06-H64/3.

Data Availability The neutron monitor data for the studied GLE event are available in the International GLE Database at https://gle.oulu.fi.

Declarations

Competing Interests The authors declare no competing interests.

References

Adriani, O., Barbarino, G.C., Bazilevskaya, G.A., Bellotti, R., Boezio, M., et al.: 2017, Ten years of PAMELA in space. *Riv. Nuovo Cimento* **40**, 473. DOI.

Aguilar, M., Ali Cavasonza, L., Ambrosi, G., Arruda, L., Attig, N., et al.: 2021, The Alpha Magnetic Spectrometer (AMS) on the international space station: part II – results from the first seven years. *Phys. Rep.* **894**, 1. DOI.

Alken, P., Thébault, E., Beggan, C.D., Amit, H., Aubert, J., et al.: 2021, International Geomagnetic Reference Field: the thirteenth generation. *Earth Planets Space* **73**. DOI.

Aster, R.C., Borchers, B., Thurber, C.H.: 2005, *Parameter Estimation and Inverse Problems*, Elsevier, New York. ISBN 0-12-065604-3.

Bieber, J.W., Evenson, P.A.: 1995, Spaceship Earth - an optimized network of neutron monitors. In: *Proc. of 24th ICRC Rome, Italy, 28 August - 8 September 1995* **4**, 1316.

Bombardieri, D.J., Duldig, M.L., Michael, K.J., Humble, J.E.: 2006, Relativistic proton production during the 2000 July 14 solar event: the case for multiple source mechanisms. *Astrophys. J.* **644**, 565.

Bombardieri, D.J., Duldig, M.L., Humble, J.E., Michael, K.J.: 2008, An improved model for relativistic solar proton acceleration applied to the 2005 January 20 and earlier events. *Astrophys. J.* **682**, 1315. DOI.

Bütikofer, R.: 2018a, Cosmic ray particle transport in the Earth's magnetosphere. In: *Solar Particle Radiation Storms Forecasting and Analysis, the HESPERIA HORIZON 2020 Project and Beyond* **79**, Springer, Cham. ISBN 978-3-319-60051-2. Chapter 5.

Bütikofer, R.: 2018b, Ground-based measurements of energetic particles by neutron monitors. In: *Solar Particle Radiation Storms Forecasting and Analysis, the HESPERIA HORIZON 2020 Project and Beyond* **95**, Springer, Cham. ISBN 978-3-319-60051-2. Chapter 6.

Caballero-Lopez, R.A., Manzano, R.: 2022, Analysis of the solar cosmic-ray spectrum during ground-level enhancements. *Adv. Space Res.* **70**, 2602. DOI.

Carmichael, H.: 1964, *IQSY Instruction Manual*, Deep River, Canada.

Cramp, J.L., Duldig, M.L., Flückiger, E.O., Humble, J.E., Shea, M.A., Smart, D.F.: 1997, The October 22, 1989, solar cosmic ray enhancement: an analysis of the anisotropy and spectral characteristics. *J. Geophys. Res.* **102**, 24237. DOI. ADS.

Dennis, J.E., Schnabel, R.B.: 1996, *Numerical Methods for Unconstrained Optimization and Nonlinear Equations*, Prentice-Hall, Englewood Cliffs. ISBN 13-978-0-898713-64-0.

Dorman, L.: 2004, *Cosmic Rays in the Earth's Atmosphere and Underground*, Kluwer Academic, Dordrecht. ISBN 1-4020-2071-6.

Engl, H.W., Hanke, M., Neubauer, A.: 1996, *Regularization of Inverse Problems*, Kluwer Academic, Dordrecht. ISBN 0792341570, 9780792341574.

Gaisser, T., Engel, R., Resconi, E.: 2016, *Cosmic Rays and Particle Physics*, Cambridge University Press, Cambridge. ISBN 9781139192194.

Guo, J., Li, X., Zhang, J., Dobynde, M.I., Wang, Y., Xu, Z., Berger, T., Semkova, J., Wimmer-Schweingruber, R.F., Hassler, D.M., Zeitlin, C., Ehresmann, B., Matthiä, D., Zhuang, B.: 2023, The First Ground Level Enhancement Seen on Three Planetary Surfaces: Earth, Moon, and Mars. *Geophys. Res. Lett.* **50**. DOI.

Hayakawa, H., Koldobskiy, S., Mishev, A., Poluianov, S., Gil, A., Usoskina, I., Usoskin, I.: 2024, Revision of the strongest solar energetic particle event of 23 February 1956 (GLE #5) based on the rediscovered original records. *Astron. Astrophys.* **684**, A46. DOI. ADS.

Himmelblau, D.M.: 1972, *Applied Nonlinear Programming*, McGraw-Hill(Tx). ISBN 978-0070289215.

Huber, R.: 2019, *Variational Regularization for Systems of Inverse Problems: Tikhonov Regularization with Multiple Forward Operators*, Springer, Wiesbaden. ISBN 9783658253899.

Johansen, T.A.: 1997, On Tikhonov regularization, bias and variance in nonlinear system identification. *Automatica* **33**, 441. DOI.

Kocharov, L., Pohjolainen, S., Mishev, A., Reiner, M.J., Lee, J., Laitinen, T., Didkovsky, L.V., Pizzo, V.J., Kim, R., Klassen, A., Karlicky, M., Cho, K.-S., Gary, D.E., Usoskin, I., Valtonen, E., Vainio, R.: 2017, Investigating the origins of two extreme solar particle events: proton source profile and associated electromagnetic emissions. *Astrophys. J.* **839**, 79. DOI.

Kocharov, L., Mishev, A., Riihonen, E., Vainio, R., Usoskin, I.: 2023, A comparative study of ground level enhancement events of solar energetic particles. *Astrophys. J.* **958**, 122. DOI.

Koldobskiy, S., Mishev, A.: 2022, Fluences of solar energetic particles for last three GLE events: comparison of different reconstruction methods. *Adv. Space Res.* **70**, 2585. DOI.

Koldobskiy, S.A., Bindi, V., Corti, C., Kovaltsov, G.A., Usoskin, I.G.: 2019, Validation of the neutron monitor yield function using data from AMS-02 experiment 2011 – 2017. *J. Geophys. Res. Space Phys.* **124**, 2367. DOI.

Koldobskiy, S., Raukunen, O., Vainio, R., Kovaltsov, G.A., Usoskin, I.: 2021, New reconstruction of event-integrated spectra (spectral fluences) for major solar energetic particle events. *Astron. Astrophys.* **647**, A132. DOI. ADS.

Kudela, K., Bučik, R., Bobik, P.: 2008, On transmissivity of low energy cosmic rays in disturbed magnetosphere. *Adv. Space Res.* **42**, 1300. DOI.

Larsen, N., Mishev, A.: 2024, Relationship Between NM Data and Radiation Dose at Aviation Altitudes During GLE Events. *Space Weather* **22**. DOI.

Larsen, N., Mishev, A., Usoskin, I.: 2023, A new open-source geomagnetosphere propagation tool (OTSO) and its applications. *J. Geophys. Res. Space Phys.* **128**, e2022JA031061. DOI.

Leonov, A.S., Yagola, A.G.: 1998, Special regularizing methods for ill-posed problems with sourcewise represented solutions. *Inverse Probl.* **14**, 1539. DOI.

Levenberg, K.: 1944, A method for the solution of certain non-linear problems in least squares. *Q. Appl. Math.* **2**, 164.

Marquardt, D.: 1963, An algorithm for least-squares estimation of nonlinear parameters. *SIAM J. Appl. Math.* **11**, 431.

Matzka, J., Stolle, C., Yamazaki, Y., Bronkalla, O., Morschhauser, A.: 2021, The geomagnetic kp index and derived indices of geomagnetic activity. *Space Weather* **19**, e2020SW002641. DOI.

Miroshnichenko, L.: 2015, *Solar Cosmic Rays*, Springer, Switzerland. ISBN 978-3-319-09428-1. DOI.

Miroshnichenko, L.I.: 2018, Retrospective analysis of GLEs and estimates of radiation risks. *J. Space Weather Space Clim.* **8**, A52. DOI.

Mishev, A.L.: 2023, Application of the global neutron monitor network for assessment of spectra and anisotropy and the related terrestrial effects of strong SEPs. *J. Atmos. Sol.-Terr. Phys.* **243**, 106021. DOI.

Mishev, A., Poluianov, S.: 2021, About the altitude profile of the atmospheric cut-off of cosmic rays: new revised assessment. *Sol. Phys.* **296**, 129. DOI.
Mishev, A., Usoskin, I.: 2016a, Analysis of the ground level enhancements on 14 July 2000 and on 13 December 2006 using neutron monitor data. *Sol. Phys.* **291**, 1225.
Mishev, A., Usoskin, I.: 2016b, Erratum to: Analysis of the ground level enhancements on 14 July 2000 and on 13 December 2006 using neutron monitor data. *Sol. Phys.* **291**, 1579.
Mishev, A., Usoskin, I.: 2020, Current status and possible extension of the global neutron monitor network. *J. Space Weather Space Clim.* **10**. DOI.
Mishev, A., Usoskin, I., Raukunen, O., Paassilta, M., Valtonen, E., Kocharov, L., Vainio, R.: 2018, First analysis of GLE 72 event on 10 September 2017: spectral and anisotropy characteristics. *Sol. Phys.* **293**, 136. DOI.
Mishev, A.L., Koldobskiy, S.A., Kovaltsov, G.A., Gil, A., Usoskin, I.G.: 2020, Updated neutron-monitor yield function: bridging between in situ and ground-based cosmic ray measurements. *J. Geophys. Res. Space Phys.* **125**, e2019JA027433. DOI.
Mishev, A.L., Koldobskiy, S.A., Kocharov, L.G., Usoskin, I.G.: 2021, GLE # 67 Event on 2 November 2003: an Analysis of the Spectral and Anisotropy Characteristics Using Verified Yield Function and Detrended Neutron Monitor Data. *Sol. Phys.* **296**. DOI.
Mishev, A.L., Kocharov, L.G., Koldobskiy, S.A., Larsen, N., Riihonen, E., Vainio, R., Usoskin, I.G.: 2022, High-resolution spectral and anisotropy characteristics of solar protons during the GLE N°73 on 28 October 2021 derived with neutron-monitor data analysis. *Sol. Phys.* **297**, 88. DOI. ADS.
Mishev, A.L., Koldobskiy, S.A., Larsen, N., Usoskin, I.G.: 2024, Spectra and anisotropy of solar energetic protons during GLE #65 on 28 October, 2003 and GLE #66 on 29 October, 2003. *Sol. Phys.* **299**, 24. DOI. ADS.
Nuntiyakul, W., Sáiz, A., Ruffolo, D., Mangeard, P.-S., Evenson, P., Bieber, J.W., Clem, J., Pyle, R., Duldig, M.L., Humble, J.E.: 2018, Bare neutron counter and neutron monitor response to cosmic rays during a 1995 latitude survey. *J. Geophys. Res. Space Phys.* **123**, 7181. DOI.
Poluianov, S., Batalla, O.: 2022, Cosmic-ray atmospheric cutoff energies of polar neutron monitors. *Adv. Space Res.* **70**, 2610. DOI. ADS.
Poluianov, S., Usoskin, I., Mishev, A., Moraal, H., Kruger, H., Casasanta, G., Traversi, R., Udisti, R.: 2015, Mini neutron monitors at Concordia Research Station, Central Antarctica. *J. Astron. Space Sci.* **32**, 281. DOI. ADS.
Poluianov, S.V., Usoskin, I.G., Mishev, A.L., Shea, M.A., Smart, D.F.: 2017, GLE and sub-GLE redefinition in the light of high-altitude polar neutron monitors. *Sol. Phys.* **292**, 176. DOI. ADS.
Poluianov, S., Batalla, O., Mishev, A., Koldobskiy, S., Usoskin, I.: 2024, Two new sub-GLEs found in data of neutron monitors at South Pole and Vostok: on 09 June 1968, and 27 February 1969. *Sol. Phys.* **299**, 6. DOI. ADS.
Raukunen, O., Vainio, R., Tylka, A.J., Dietrich, W.F., Jiggens, P., Heynderickx, D., Dierckxsens, M., Crosby, N., Ganse, U., Siipola, R.: 2018, Two solar proton fluence models based on ground level enhancement observations. *J. Space Weather Space Clim.* **8**, A04. DOI. ADS.
Reames, D.V.: 1995, Solar energetic particles: a paradigm shift. *Rev. Geophys.* **33**, 585. DOI.
Simpson, J.A.: 2000, The cosmic ray nucleonic component: the invention and scientific uses of the neutron monitor – (keynote lecture). *Space Sci. Rev.* **93**, 11. DOI.
Smart, D.F., Shea, M.A.: 2009, Fifty years of progress in geomagnetic cutoff rigidity determinations. *Adv. Space Res.* **44**, 1107. DOI.
Smith, C.W., L'Heureux, J., Ness, N.F., Acuña, M.H., Burlaga, L.F., Scheifele, J.: 1998, The ace magnetic fields experiment. *Space Sci. Rev.* **86**, 613. DOI.
Strauss, D.T., Poluianov, S., van der Merwe, C., Krüger, H., Diedericks, C., Krüger, H., Usoskin, I., Heber, B., Nndanganeni, R., Blanco-Ávalos, J., García-Tejedor, I., Herbst, K., Caballero-Lopez, R., Moloto, K., Lara, A., Walter, M., Giday, N.M., Traversi, R.: 2020, The mini-neutron monitor: a new approach in neutron monitor design. *J. Space Weather Space Clim.* **10**, 39. DOI. ADS.
Tikhonov, A.N., Goncharsky, A.V., Stepanov, V.V., Yagola, A.G.: 1995, *Numerical Methods for Solving ill-Posed Problems*, Kluwer Academic, Dordrecht. ISBN 978-90-481-4583-6.
Tsyganenko, N.A.: 1989, A magnetospheric magnetic field model with a warped tail current sheet. *Planet. Space Sci.* **37**, 5.
Tylka, A.J., Dietrich, W.F.: 2009, A new and comprehensive analysis of proton spectra in Ground-Level Enhanced (GLE) solar particle events. In: *Proc. 31th Int. Cosmic Ray Conf.*, Lodz.
Usoskin, I.G., Gil, A., Kovaltsov, G.A., Mishev, A.L., Mikhailov, V.V.: 2017, Heliospheric modulation of cosmic rays during the neutron monitor era: calibration using PAMELA data for 2006 – 2010. *J. Geophys. Res.* **122**, 3875. DOI. ADS.
Usoskin, I., Koldobskiy, S., Kovaltsov, G.A., Gil, A., Usoskina, I., Willamo, T., Ibragimov, A.: 2020, Revised GLE database: fluences of solar energetic particles as measured by the neutron-monitor network since 1956. *Astron. Astrophys.* **640**, 2038272. DOI.

van Wieringen, W.N.: 2015, Lecture notes on ridge regression. arXiv e-prints. arXiv. ADS.
Vashenyuk, E.V., Balabin, Y.V., Perez-Peraza, J., Gallegos-Cruz, A., Miroshnichenko, L.I.: 2006, Some features of the sources of relativistic particles at the Sun in the solar cycles 21 – 23. *Adv. Space Res.* **38**, 411. DOI.
Waterfall, C.O.G., Dalla, S., Raukunen, O., Heynderickx, D., Jiggens, P., Vainio, R.: 2023, High Energy Solar Particle Events and Their Relationship to Associated Flare, CME and GLE Parameters. *Space Weather* **21**. DOI.
Xaplanteris, L., Livada, M., Mavromichalaki, H., Dorman, L., Georgoulis, M.K., Sarris, T.E.: 2021, Improved Approach in the Coupling Function Between Primary and Ground Level Cosmic Ray Particles Based on Neutron Monitor Data. *Sol. Phys.* **296**. DOI.
Yagola, A.G., Leonov, A.S., Titarenko, V.N.: 2002, Data errors and an error estimation for ill-posed problems. *Inverse Probl. Eng.* **10**, 117. DOI.